Polymer 51 (2010) 5929–5941

Contents lists available at ScienceDirect

Polymer

journal homepage: www.elsevier.com/locate/polymer

Structurally isomeric monomers Directed copolymerization of polybenzimidazoles and their properties

Arindam Sannigrahi, Sandip Ghosh, Sudhangshu Maity, Tushar Jana*

School of Chemistry, University of Hyderabad, Hyderabad, India

ARTICLE INFO

Article history:
Received 13 August 2010
Received in revised form
6 October 2010
Accepted 10 October 2010
Available online 16 October 2010

Keywords:
Polybenzimidazole
Monomer isomeric effect
Proton exchange membrane fuel cell

ABSTRACT

Three different series of pyridine based polybenzimidazole (PyPBI) random copolymers consisting of meta-para pyridine linkages were synthesized from various stoichiometric mixtures of meta (2,4; 2,6 and 3,5) and para (2, 5) structure pyridine dicarboxylic acids (PDA) with 3, 3', 4, 4'- tetra-aminobiphenyl (TAB) by solution polycondensation in polyphosphoric acid (PPA). The influences of the structural isomers of PDA on the PyPBI copolymerization and properties were elucidated by characterizing the resulting copolymers. The solubility of PDA monomers in PPA and the overall monomer concentration in the polymerization were found to be the deciding factors. The higher molecular weight PyPBI were obtained for higher para content copolymers due to the low solubility of para PDA in PPA. The introduction of para structure had enhanced the conjugation along the polymer chain. NMR study showed that the reactivity ratio of para PDA was not identical for all the three sets of PyPBI copolymers, it varied upon the positions of the dicarboxylic acids in the pyridine ring of meta PDAs (structural isomeric effect) with which 2,5 PDA is forming the copolymer. Introduction of para structure and meta PDAs structural isomers affected the thermal stability, flexibility and the photophysical properties of the PyPBI copolymers.

1. Introduction

Recently, polymer electrolyte membrane fuel cells (PEMFC) operating at high temperature have attracted a huge amount of attention owing to their numerous advantages compared to PEMFC operating at lower than 100 °C [1,2]. Several efforts have been made to develop the variety of polymer membranes which can operate above 120 °C in their polyelectrolyte state [3,4]. Phosphoric acid (PA) doped polybenzimidazole (PBI) membrane is found to be the most attractive and promising for the use in high temperature PEMFC [5,6]. To date a large variety of PBI polymers have been synthesized and studied in the literature [7,8]. Therefore, synthesis of PBI polymers with a variety of structures still remains an important area of investigation for the polybenzimidazole chemistry.

The commercially available PBI, poly [2,2′–(1,3–phenylene)–5,5′–benzimidazole] (known as m-PBI) [9] is the most widely used among all PBI polymers. Other varieties include poly [2,2′–(1,4–phenylene)–5,5′–benzimidazole] (known as p-PBI) [10], poly(2,5 benzimidazole) (AB–PBI) [11], pyridine based PBI homopolymer [12], sulfonated PBI [13], hyperbranched polybenzimidazole (HPBI) [14], naphthalene based PBI [15], fluorinated PBI [16], meta and para PBI copolymer [17], PBI with sulfone or sulfonic acid groups [18] in the backbone etc. PBI is a basic polymer ($pK_a \sim 5.25$) and possesses both proton donor (–NH–) and proton acceptor (–N=) hydrogen bonding sites which exhibit specific interactions with the polar solvents [19–21] and forms miscible blends with variety of polymers [22–24]. Polybenzimidazole has excellent thermal and chemical resistance, fire retarding capacity, insulating properties as well as having good textile fiber forming ability [25] However, the poor solubility of PBIs resulting from the highly rigid polymer backbones and the strong intra-interchain hydrogen bonding interactions makes them hard to process [19,20,26]. Several attempts have been made through the modification of the polymer backbone as well as side chain to solve the solubility issues. Many investigators have incorporated flexible spacers such as methylene and aryl methylenes, arylamide and ether linkages in the polymer backbone [27–29].

Phosphoric acid (PA) doped PBI is most interesting because of its amphoteric and strong thermal stability nature as well as low vapour pressure at elevated temperatures. It forms dynamic hydrogen bond networks in which protons can readily transfer by hydrogen bond breaking and forming processes [7,30]. Various approaches have been attempted so far for the fabrication of PA doped PBI membranes; these include casting PBI membrane by dissolving of PBI in dimethyl acetamide (DMAc) solvent followed by soaking of the membrane in

* Corresponding author. Tel.: +91 40 23134808; fax: +91 40 23012460.
E-mail addresses: tjsc@uohyd.ernet.in, tjscuoh@gmail.com (T. Jana).

0032-3861/$ – see front matter © 2010 Elsevier Ltd. All rights reserved.
doi:10.1016/j.polymer.2010.10.013

phosphoric acid (PA) [7,31,32], via sol–gel process by direct casting of the high molecular weight PBI solution in polyphosphoric acid (PPA) [12,33] and from thermoreversible gel of PBI in PA [34]. The major challenge for the fabrication of PA doped PBI is to get a membrane with high acid doping level and moderately good mechanical stability. If the acid content of the membrane is too high it forms soft plastic type material which does not have enough mechanical strength to form a membrane [7,35]. To get a superior quality membrane, a compromise between these two important parameters (acid loading and mechanical stability) has to be maintained. Different methods have been explored to improve the acid loading without compromising on the mechanical strength or vice versa. These include synthesis of new PBI polymers having a variety of polymer backbone structures [12–17], high molecular weight PBI polymer synthesis by copolymerization [17], introduction of cross-linkage between the polymer chains [35,36], incorporation of inorganic fillers in the PBI matrix [37,38].

Recently, we have shown that the high molecular weight PBI synthesis depends upon the solubility of the monomers in the reaction medium. We have demonstrated that the molecular weight of PBI polymer can be readily tuned by choosing the carboxylic acid architecture appropriately. The change in the molecular weight of PBI by changing the monomer structure also alters the molecular properties of the PBI copolymer. We have found that low solubility of para structure dicarboxylic acid (terephthalic acid) in polyphosphoric acid (PPA) medium, which is the reaction medium, is the dominating factor for resulting the higher molecular weight polymer [17]. In order to universalize the solubility and architectural effects of dicarboxylic acid monomers on the PBIs copolymerization and properties, we have chosen the various structural isomers of pyridine dicarboxylic acid (PDA) monomers in the present study. In addition, it is expected that introduction of pyridine ring will enhance the basic nature of the resulting PBI which may facilitates the higher PA loading. The current study is also encouraged by an earlier report on pyridine containing polyimides which demonstrated very interesting thermal and photophysical properties [39].

In the present study, we report synthesis, characterization and studies of a series of pyridine based polybenzimidazole (PyPBI) random copolymers. The synthesized polymers are characterized by determining inherent viscosity (I.V.) as a measurement of polymer molecular weight, thermo gravimetric analysis (TGA) for the thermal stability, dynamic mechanical analyzer (DMA) for the thermal transitions. Fourier transforms infrared (FT-IR) and Raman and proton NMR techniques are used to establish the polymer structure. Also, spectroscopic studies such as absorption and fluorescence are carried out to demonstrate the effect of copolymerization on the photophysical properties.

2. Experimental

2.1. Materials

3, 3', 4, 4'- tetra-aminobiphenyl (TAB, polymer grade) and polyphosphoric acid (PPA, 115%) were purchased from Sigma–Aldrich. 2,4 pyridine dicarboxylic acid (98%), 2,5 pyridine dicarboxylic acid (98%), 2,6 pyridine dicarboxylic acid (99%) and 3,5 pyridine dicarboxylic acid (98%) were purchased from Sigma–Aldrich and purified by recrystallization in water and dil HCL (9:1) mixture prior to use. Dimethyl acetamide (DMAc, HPLC grade) was purchased from Qualigens-India. Sulfuric acid (98%) was purchased from Merck, India. The NMR solvent dimethyl sulfoxide (DMSO-d_6) was obtained from Acros Organics. All the solvents were used without further purification.

2.2. Polymer synthesis

Equal mols of pyridine dicarboxylic acids (2, 4 or 2, 5 or 2, 6 or 3, 5 PDAs) and TAB were taken into a three neck flask with polyphosphoric acid (PPA) for homopolymers synthesis. 2, 4; 2,6 and 3,5 pyridine dicarboxylic acids (PDA) were used to prepare meta oriented pyridine polybenzimidazole (PyPBI) and 2,5 was used to prepare para oriented pyridine polybenzimidazole (PyPBI) homo polymer, respectively. The two carboxylic acid groups in the 2,5 PDA are positioned opposite to each other thus it is called para oriented while in other cases carboxylic acids groups positioned one carbon apart are called meta oriented. Three sets of different random PyPBI copolymers (2,6 and 2,5), (3,5 and 2,5) and (2,4 and 2,5) were synthesized by varying the mol fraction of the diacids (meta and para) in the reaction mixture from 10% to 90% but maintaining the total mol of diacids equal to the mol of TAB taken in the reaction mixture along with PPA. The polymerization is presented in Scheme 1. Total monomer concentrations were gradually decreased with increasing 2,5 PDA (para) mol fraction in the mixtures. The reaction mixture was placed in a digitally temperature controlled oil bath .The reaction mixtures were stirred by an overhead mechanical stirrer continuously in the nitrogen atmosphere at 190–210 °C for ~24 h. The viscosity of the reaction mixture increased as the polymerization proceeds and resulted in a dark brown colour at the end of the polymerization. The PBI polymers were isolated, neutralized with sodium carbonate, washed thoroughly with water and dried in a vacuum oven at 100 °C for 24 h. The dried polymers were kept in vacuum desiccators for further characterizations.

2.3. Viscosity

The viscosity measurements of the polymer solutions in H_2SO_4 (98%) were carried out at 30 °C in a constant temperature water bath using a Cannon Ubbelohde capillary dilution viscometer (model F725). The inherent viscosity (I.V.) values were calculated from the flow time data. For all the flow time measurements 0.2 g/dL polymer solution in H_2SO_4 (98%) was used. The molecular weight of PBI in the related literature has been expressed in terms of I.V., measured from sulfuric acid solution [10,25].

2.4. IR spectra

The IR spectra of the PyPBI homo and copolymers films were recorded on a (Nicolet 5700 FTIR) FT-IR spectrometer. The PyPBI films of thickness 30–40 μm were made from DMAc solutions (2% w/v) of the polymers. The resolution of the IR spectrometer is about 4 cm^{-1}.

2.5. Raman spectra

The Raman spectra were recorded using a Bruker Opus Raman spectrometer equipped with 1064 nm diode laser. The exposure time was 35 s. The resolution was about 4 cm^{-1}.

2.6. NMR spectroscopy

All the NMR spectra were recorded using Bruker AV 400 MHz NMR spectrometer at room temperature using DMSO-d_6 as NMR solvent.

2.7. Thermal study

Thermogravimetric and differential thermal analysis (TG-DTA) were carried out on a (Netzsch STA 409 PC) TG-DTA instrument from 30 to 800 °C with a scanning rate of 10 °C/minute in presence of nitrogen gas flow.

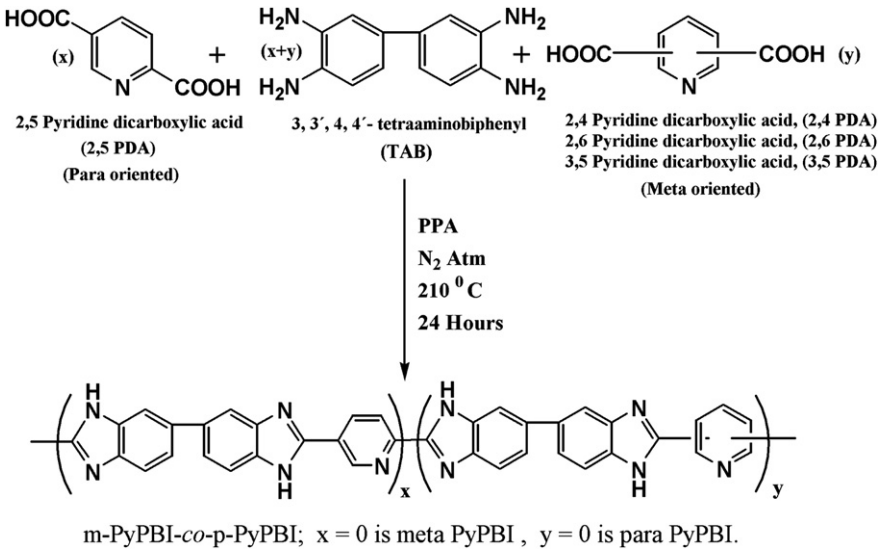

Scheme 1. Synthesis of m-Pyridinepolybenzimidazole-*co*-p-Pyridinepolybenzimidazole (m-PyPBI-*co*-p-PyPBI).

2.8. Mechanical property study

The mechanical properties of the PyPBI films were measured using a dynamic mechanical analyzer (DMA) (TA Instruments, model Q-800). PyPBI films casted from DMAc (2% w/v) solution of the polymers were boiled repeatedly with distilled water for washing and finally dried in oven at 100 °C for 24 h. Films of 25 mm × 5 mm × 0.05 mm (L × W × T) dimensions were cut and clamped on the films tension clamp of the pre-calibrated instrument. The samples were annealed at 150 °C for 30 min and then scanned from 150 °C to 500 °C at heating rate of 4 °C/min. The storage modulus (E′), loss modulus (E″) and tan δ values were measured at a constant linear frequency of 5 Hz with preload force of 0.01 N.

2.9. Absorption and fluorescence spectroscopy

Electronic absorption spectra were recorded on a Cary-100 Bio (VARIAN) UV–visible spectrometer. Steady-state fluorescence emission spectra were recorded on a Jobin Yvon Horiba spectro-fluorimeter (Model Fluoromax-4). PBI samples were dissolved in dimethyl acetamide (DMAc) and the spectra were recorded.

3. Results and discussion

3.1. Synthesis and molecular weight control

We have synthesized three series of m-Pyridine poly-benzimidazole-*co*-p-Pyridinepolybenzimidazole random copoly-mers (m-PyPBI-*co*-p-PyPBI) and the polymer backbone structures are shown in Scheme1. Pyridine-dicarboxylic acid (PDA) has four different meta and para isomers (2,4; 2,5; 2,6 and 3,5) based on there positions in the pyridine ring (Scheme 2). In this article our goal is to prepare meta–para PBI random copolymers based on PDA monomers. Since PDA has three meta (2,4; 2,6 and 3,5) and one para (2,5) isomers, hence we have synthesized three different series of meta–para PyPBI random copolymers. These are 2,4(m)-PyPBI-*co*-2,5(p)- PyPBI; 2,6(m)-PyPBI-*co*-2,5(p)-PyPBI and 3,5(m)-PyPBI-*co*-2,5(p)-PyPBI. Polymer backbone structure of these three different sets of PDA based random copolymers and three different sets of PDAs are shown in Scheme1 and Scheme 2, respectively. We have carried out the copolymerization by varying the meta and para contents (mol %) in the copolymers from 10% to 90% in the initial reaction mixture. Also, three different meta (2,4; 2,6 and 3,5)

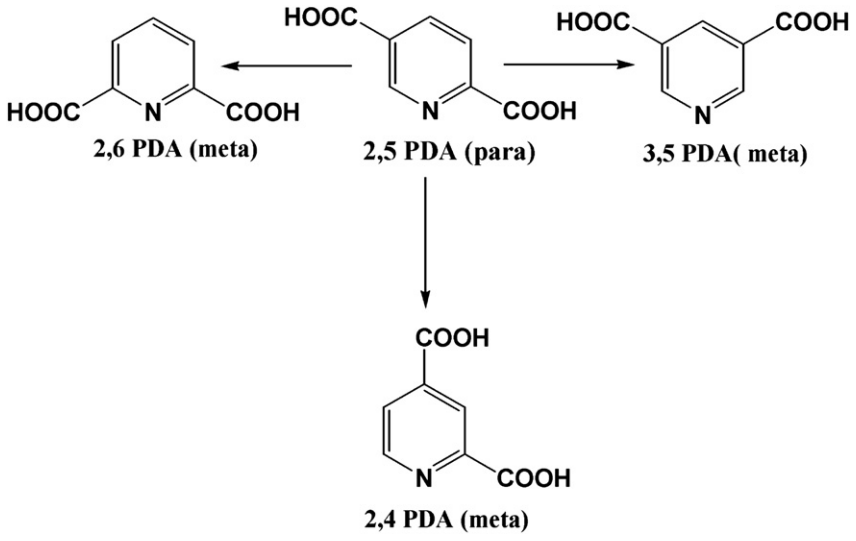

Scheme 2. Three different sets of pyridine dicarboxylic acid (PDA) monomers.

homopolymers and para(2,5) homopolymer were prepared by taking the respective diacid with the TAB. In all the polymerization reactions the stoichiometry of TAB and the diacids (meta + para) were maintained as equal mols and the reaction conditions for all the polymerizations were similar except the initial monomer concentrations in the reaction mixtures. In case of condensation polymerization higher monomer concentration yields the higher molecular weight polymers. However, the solubility of the monomer in the reaction mixture dictates the amount of monomers which can be taken in the reaction mixture. In case of poor solubility of the monomer, a lower monomer concentration needs to be taken; otherwise the presence of insoluble monomers disfavors the polymerization reaction and resulting lower molecular weight polymer. We have carried out the polymerization reaction with a gradual decrease in monomer concentration with increasing para content in the copolymer and higher monomer concentrations are used for meta PyPBI (Table 1). Earlier, it has been shown that the para structure PBI can be made with high molecular weight if the lower monomer concentration is employed owing to the lower solubility of para oriented dicarboxylic acid [17,29,40].

The molecular weight of the PBI family of polymers are generally expressed in terms of their inherent viscosity (I.V.) [10,25]. The higher I.V. attributes higher molecular weight. Table 1 represents the I.V. values of all the copolymer for all three series. Table 1 clearly demonstrates that low monomer concentration is required for higher para content in all the cases to obtain higher molecular weight polymer. In fact our attempts to prepare higher para content polymers with monomer concentration similar to meta polymer yielded very low I.V. polymers. These observations clearly prove the fact that low solubility of para oriented PDA demands the lower monomer concentration in the polymerization mixture. Hence the monomer concentration is an important parameter which needs to be adjusted to produce bigger PBI polymers.

Table 1 exhibits that the molecular weight of all the three sets of m-PyPBI-*co*-p-PyPBI polymers increases with increasing para content in the polymer backbone. This observation is similar with our previous observation in case of m-PBI-*co*-p-PBI, although in the previous case the increase is much more than the current one. Earlier, we have shown that the solubility of the monomers in PPA (polymerization medium) plays a vital role for the synthesis of high molecular weight PBI [17]. It has been found that para oriented dicarboxylic acid are less soluble in PPA medium because acid groups are probably unable to form the internal dimmers through hydrogen bonding interaction between carboxylic groups of the same acids or coming from two different molecules of the acid [41,42]. Hence 2,5 PDA (para) is less soluble in PPA medium than all other PDAs. The lower solubility of para dicarboxylic acid monomer forces the growing polymer chain oligomers to undergo an unusual heterogeneous reaction pathway in which the oligomer ends consist of soluble TAB monomer. This reaction pathway ensures the formation of bigger molecules. We propose this reaction pathway as, first tetra amine monomer (TAB) reacts with diacids forms a species in which one end is amine and other end is acid (acid-amine terminated species). Then the acid-amine terminated species can react further with both the diacid and TAB. But since the availability of the diacid in the reaction medium is not very high owing to its poor solubility, therefore the soluble TAB will have greater chance to react with the acid-amine terminated species and it produces the amine terminated oligomeric chains. This oligomeric chain can only react with diacids since it is amine terminated. Hence more diacid molecules will come to the solution from its undissolved solid state and react with amine terminated oligomeric chain. The similar observation we have made in our previous studies. The less distinct increase of molecular weight in the current copolymers compared to our previous report is due to the better solubility of 2,5 PDA monomer than the terephthalic acid (TPA) owing to the presence of pyridine nitrogen in 2,5 PDA.

Table 1
Various reaction parameters and molecular weight of m-PyPBI-*co*-p-PyPBI random copolymers.

Copolymer	Para Content (mol%)	Monomer Concentration (Weight %)	Inherent viscosity (dL/g)
2,6(m)-PyPBI-co–2,5(p)–PyPBI	0	9.00	0.85
	10	8.75	1.07
	25	8.50	0.99
	50	8.25	1.02
	75	8.00	1.25
	90	7.75	1.21
	100	6.00	1.75
3,5(m)-PyPBI–co–2,5(p)–PyPBI	0	12.00	0.55
	10	11.75	0.72
	25	11.50	0.71
	50	11.25	1.29
	75	11.00	1.47
	90	10.75	1.57
	100	6.00	1.75
2,4(m)-PyPBI–co–2,5(p)–PyPBI	0	9.00	0.60
	10	8.75	0.75
	25	8.50	1.11
	50	8.25	0.94
	75	8.00	1.02
	90	7.75	1.33
	100	6.00	1.75

3.2. IR and Raman spectroscopy

FT-IR spectra of all PyPBI homo and random copolymers are recorded from 30 to 40 μm thin polymer films made from the dilute solution (2% w/v) of the polymers in dimethyl acetamide (DMAc). Fig. 1 shows the IR spectra of all the homopolymers and the 3,5(m)-PyPBI-*co*-2,5(p)-PyPBI copolymer samples with different para mol %. The IR spectra of the other two sets of copolymers are shown in Supporting Information Figs. 1 and 2. All the films are boiled in hot water thoroughly and dried in vacuum oven at 100 °C for two days prior to recording of the IR spectra. The absence of C–H stretching of $-CH_3$ at 2940 cm^{-1} due to DMAc in the IR spectra proves the complete elimination of DMAc from the films by the above the drying process. The IR spectra of all the PyPBI homo and random copolymers are quite similar and the stretching bands are the characteristic bands of PBI. PBI polymers absorb moisture upto ~5% of their weight owing to their hygroscopic nature and therefore in all the IR spectra O–H stretching of H_2O at 3615–3620 cm^{-1} is observed (Fig. 1) [43]. The absorptions at 3415 and 3175 cm^{-1} are because of free nonhydrogen bonded N–H stretching and self-associated N–H stretching, respectively. The low intensity peak at 3063 cm^{-1} is due to the stretching modes of aromatic C–H groups (Fig. 1). The similar kind of IR spectra of PBI polymers have been already discussed earlier by several authors [22–24]. Our findings are very similar to our previous work in case of all the three sets of copolymers. The in plane ring vibration of 2,6 disubstituted benzimidazole at ~1440 cm^{-1} becomes more sharp with increasing para content (Fig. 1 and Supporting Information Figs. 1 and 2). It is evident from these spectra that the band at 1540 cm^{-1} gradually decreases with increasing para content in the polymer chain and becomes almost non existent for 100% para PyPBI. The reason behind the deviation of these stretching bands intensities is because of the different substitution in the 2nd position of the benzimidazole owing to the different polymer backbone structure (meta and para) achieved by copolymerization. It is also worth noting that in all the cases (Fig. 1 and Supporting Information Figs. 1 and 2) the peak at 1105 cm^{-1} for meta PyPBI slowly shifts towards

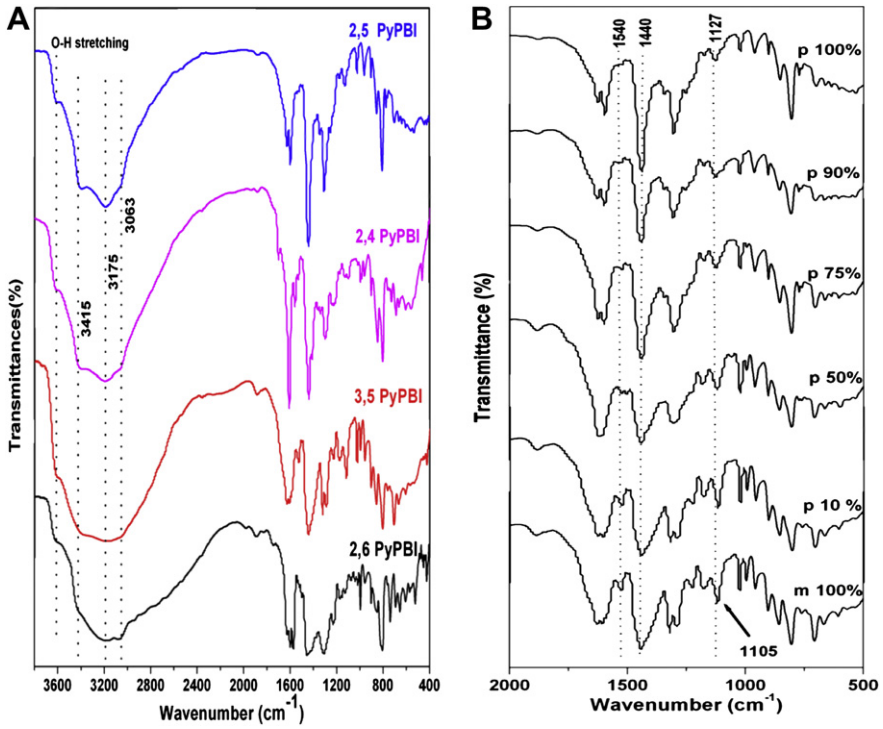

Fig. 1. FT-IR spectra of (A) all the PyPBI homo polymers and (B) 3,5(m)-PyPBI-*co*-2,5(p)-PyPBI random copolymers. The para contents are shown in the figure. The dotted lines are shown to discuss the important IR bands. The films (30 μm) obtained from 2% (w/v) DMAc solution.

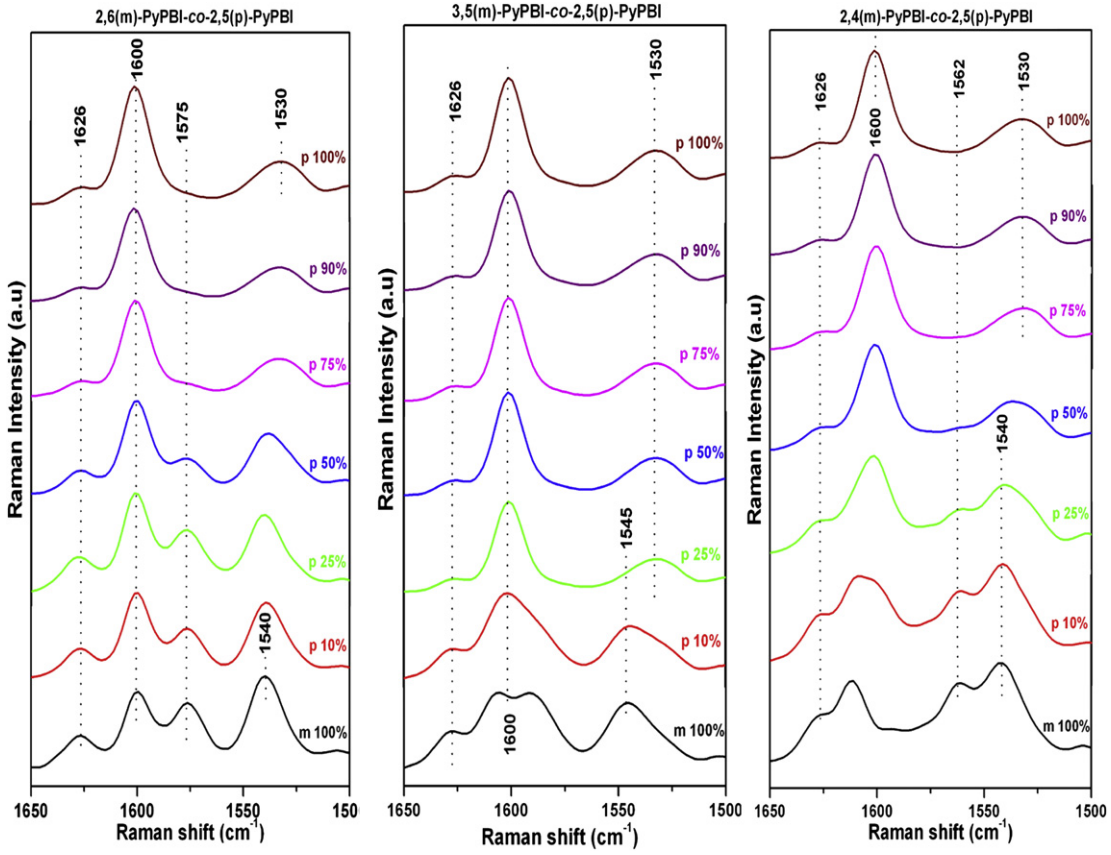

Fig. 2. Raman spectra (1650-1500 cm^{-1}) of all the three sets of random copolymers. The para content of the copolymers are shown in the figures. The important bands are indicated using dotted lines.

the higher frequency with increasing para content in the copolymer and for 100% para the band appears at 1127 cm^{-1}. This band corresponds to the N–C stretching of benzimidazole group coupled with the substitution of the α carbon atom [17,44]. The introduction of para substitution in the polymer chain brings more flexibility and symmetry in the polymer backbone and it interferes with the vibration characteristics, therefore the N–C–C coupled vibration takes place at higher frequency.

The IR studies described in the above section demonstrated the effect of copolymerization and the polymer backbone structure on the stretching of various groups. We have also studied FT-Raman spectra to understand the effect of copolymerization to a deeper extent. The use of Raman spectroscopy as a tool to study the PBI type polymer is very rare. Recently meta PBI, 2,6 PyPBI and their composites have been characterized by Raman spectroscopy [37,45]. Except for these two reports, extensive use of Raman spectroscopy to characterize PBI type polymers is not known in the literature. Raman spectra of all the PyPBI homo and copolymer are recorded from solid powder sample and represented in the Supporting information Figs. 3–6. The various bands are previously assigned and our result matches well with the previous data [37]. The most prominent bands are located between 1630 and 1500 cm^{-1} and therefore we have analyzed the Raman data by plotting the spectra between 1650 and 1500 cm^{-1} as shown in Fig. 2. All the bands in these regions are attributed to the benzimidazole ring stretching vibrations. These are the stretching of C=N and C=C bands of benzimidazole ring. The bands around 1600 cm^{-1} and 1500 cm^{-1} are due to C=N and C=C stretching of the benzimidazole ring, respectively (Fig. 2). In case of 2,6(m)-PyPBI-*co*-2,5(p)-PyPBI, the C=C stretching band at 1540 cm^{-1} (100% m) shifts towards lower wavenumber (1530 cm^{-1}) and becomes weaker with increasing para content (Fig. 2). The other C=C stretching band at 1575 cm^{-1} (100% m) slowly disappears with increasing para content and become invisible for 100% para. These observations attribute the elongation or increased conjugation of the C=C with increasing para content. The C=N stretching at 1626 and 1600 cm^{-1}also exhibit significant change with increasing para content. The band at 1626 cm^{-1} almost disappears and band at 1600 cm^{-1} becomes sharper with increasing para content (Fig. 2). This finding once again hints at the increased conjugation along the polymer backbone with increasing para content. Similar displacements and changes of the C=N and C=C stretching vibrations are also observed for other two sets [2,4(m)-*co*-2,5(p) and 3,5(m)-*co*-2,5(p)] of PyPBI random copolymers. Therefore from the Raman study it is very much clear that the conjugation along the PyPBI copolymer backbone enhances with increasing para structure in the copolymer composition. In conclusion, both IR and Raman spectroscopy study demonstrate the effect of copolymerization on the better conjugation of PyPBI random copolymers with increasing para content in the copolymer chain.

3.3. NMR studies and monomer reactivity ratio

FT-IR and Raman spectroscopy studies described in the previous section, show the isomeric effect of PDA monomers on the copolymerization and were used for the qualitative prediction of the structure of the copolymers.^{1}H-NMR is a very efficient and rapid method and has been extensively used in the past to determine the micro structure of the copolymer and the copolymers compositions very precisely. ^{1}H NMR spectra of all the samples were recorded in Bruker AV 400 MHz NMR spectrometer in DMSO-d_6 solvent. The proton NMR spectra of all the PyPBI homopolymers are shown in Fig. 3 along with their structure and the peak assignments. Fig. 4 represents the NMR spectra of all the copolymer samples of 3,5 (m)-PyPBI-*co*-2,5(p)-PyPBI random copolymers. The NMR spectra of the other two sets of copolymers [2,6(m)-PyPBI-*co*-2,5(p)-PyPBI and 2,4(m)-PyPBI-*co*-2,5(p)-PyPBI] are presented in the Supporting information Figs. 7 and 8, respectively. The peak assignments as shown in the figures are in good agreement with the anticipated chemical structure. The ^{1}H NMR spectra of PyPBI homopolymers are quite different owing to their different chemical environment (Fig. 3). The imidazole proton signals for 3,5(m)-PyPBI-*co*-2,5(p)-PyPBI denoted as H_g and H_n for the meta and para positions of the chain, are observed at around 13.60 and 13.30 ppm, respectively (Fig. 4). The downfield shift of the H_g imidazole proton from the H_n proton is because of the different chemical environment of the 3,5 meta structure compare to the 2,5 para structure. The peaks denoted by H_h (9.45) and H_i at (9.36) are for the 3,5 meta structure (3,5 PDA). The para (2,5 PDA) structure has distinguishable peak at 9.59, 8.75 and 8.35 ppm, denoted by H_q, H_p and H_o, respectively. The intensity of the characteristic meta signals (H_g, H_h and H_i) are decreasing and para responsive signals (H_n, H_q, H_p and H_o) are increasing with increasing para content in the polymer chain (Fig. 4). Similar kinds of observations are noted from the Supporting information Figs. 7 and 8 for the other two sets of PyPBI random copolymers. 2,6(m)-PyPBI-*co*-2,5(p)-PyPBI copolymers do not

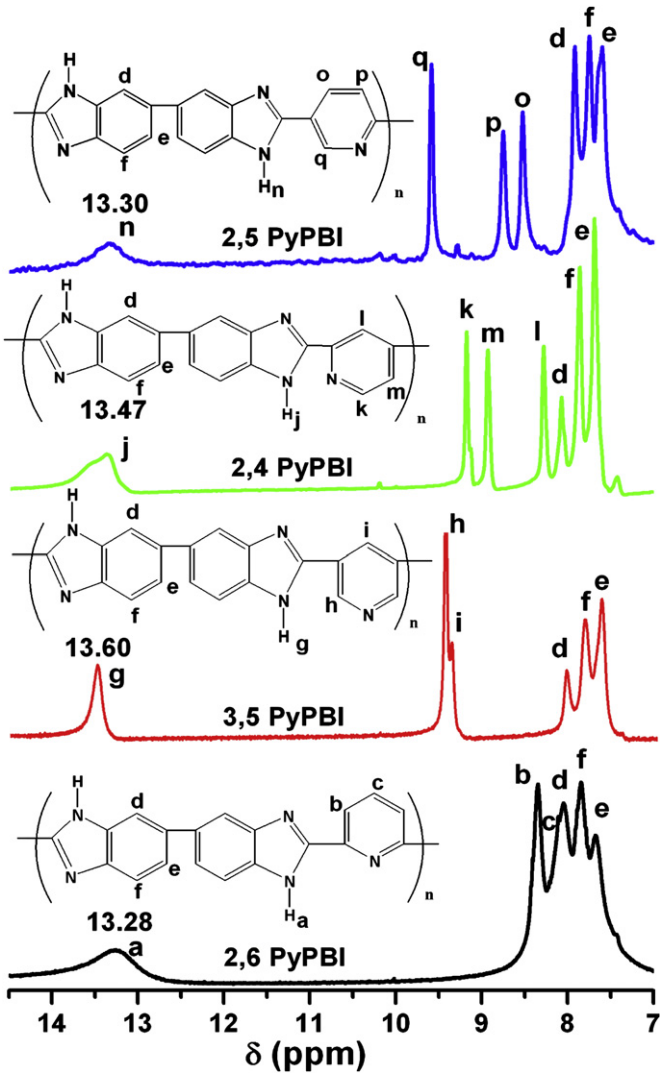

Fig. 3. Proton NMR spectra of all PyPBI homo polymers recorded in DMSO-d_6 solvent. The chemical structure and the peak assignments are also shown in the picture.

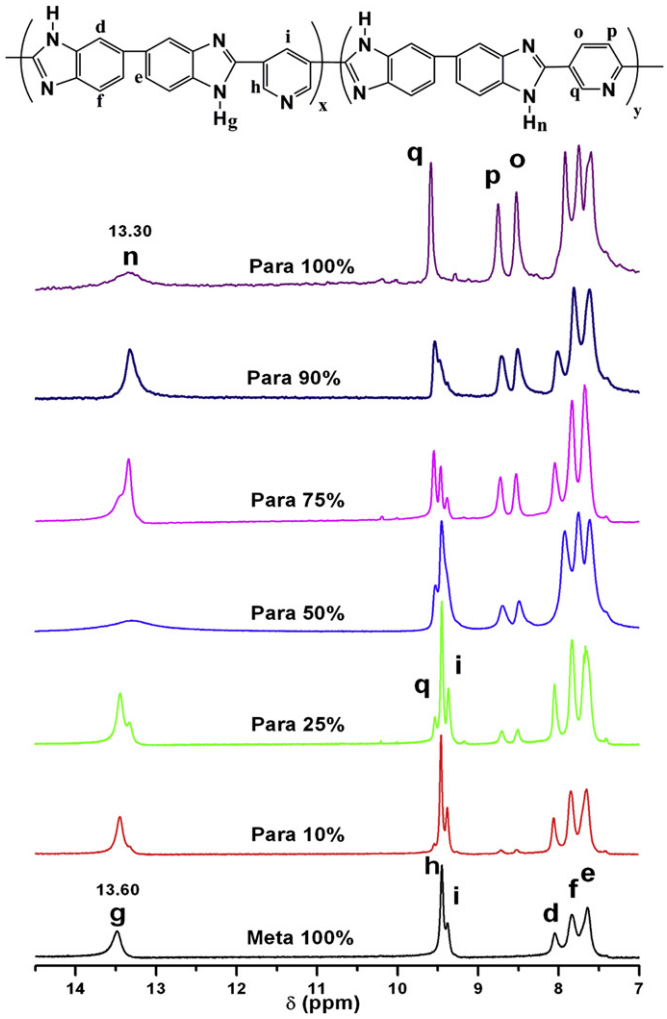

Fig. 4. The chemical structure, proton NMR spectra of all the 3,5(m)-PyPBI-*co*-2,5(p)-PyPBI copolymer and their peak assignments.

show any splitting of imidazole protons instead of that we observed a broad imidazole signals because both –NH signal appear almost in the same region (13.28 and 13.30 ppm; Fig. 3 and Supporting information Fig. 7). The other proton signals (H_q, H_p and H_o) for the para structure of this pair decreases with increasing meta content in the polymer chain. The imidazole protons signals in case of 2,4(m)-PyPBI-*co*-2,5(p)-PyPBI copolymers are splitted, denoted by H_j and H_n (Supporting Information Fig. 8). Similar to previous two sets of copolymers in this case also proton signals (H_k, H_l, H_m) for meta decreases with increasing para content in the polymer

Table 2
Comparison of expected para content of the copolymers based on 2,5 PDA feed in the reaction with measured para content calculated from proton NMR Estimated error margin is ±0.06.

Feed 2,5 PDA (Para)(mol %)	Found Para content (mol %)		
	2,6(m)-PyPBI-co-2,5(p)-PyPBI	3,5(m)-PyPBI-co-2,5(p)-PyPBI	2,4(m)-PyPBI-co-2,5(p)-PyPBI
10	23.1	15.4	12.9
25	33.3	29.0	31.4
50	47.4	53.8	50.8
75	79.4	73.8	74.3
90	93.1	87.9	88.6
100	100	100	100

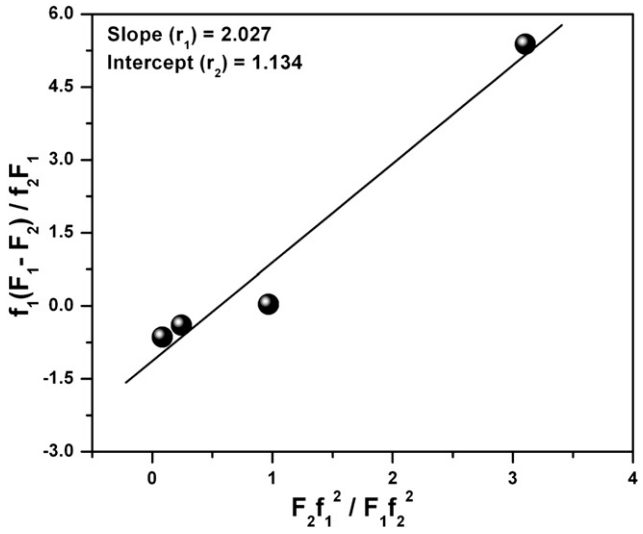

Fig. 5. Fineman–Ross Plot for calculating reactivity ratios of monomers of (2,5 PDA and 2,4 PDA) in case of 2,4(m)-PyPBI-*co*-2,5(p)-PyPBI copolymer.

chain as shown in Supporting information Fig. 8. These above observations from the ^{1}H NMR results demonstrated that in all the cases successful copolymerization have taken place and these NMR data can be utilized to determine the ratio of meta and para mol fraction in the copolymer samples.

We have calculated the % of para mol fraction in the copolymers from the integral ratio of the distinguishable proton peaks from the NMR spectrum using equation (1)–(3) for the three sets of copolymer and the results are shown in the Table 2.

$$\text{Para mol fraction (\%) for } 2,6(m)-\text{PyPBI}-co-2,5(p)-\text{PyPBI} = \frac{H_q + H_p + H_o}{H_b + H_c + H_q + H_p + H_o} \times 100 \quad (1)$$

$$\text{Para mol fraction (\%) for } 3,5(m)-\text{PyPBI}-co-2,5(p)-\text{PyPBI} = \frac{H_n + H_q + H_p + H_o}{H_g + H_n + H_q + H_p + H_o + H_h + H_i} \times 100 \quad (2)$$

$$\text{Para mol fraction (\%) for } 2,4(m)-\text{PyPBI}-co-2,5(p)-\text{PyPBI} = \frac{H_n + H_q + H_p + H_o}{H_j + H_n + H_q + H_p + H_o + H_k + H_m + H_l} \times 100 \quad (3)$$

The para content in all the three sets of PyPBI random copolymers shown in the Table 2 suggests the successful incorporation of meta and para components in the copolymer chains and the values are in good agreement with the monomer feed ratio taken in the initial reaction mixtures. Hence, it is apparent that the meta and para composition in the copolymer chains can be readily tuned by changing the molar feed ratio of meta and para monomers in the starting of the polymerization. However, a critical observation of the Table 2 data brings our attention to a moderate deviation in the para composition from the monomer feed, in particular for lower

Table 3
Reactivity ratio values calculated from Fineman–Ross method. r_1 and r_2 are the reactivity ratio for para (2,5 PDA) and meta (2,6; 3,5; 2,4 PDAs), respectively.

	r_1	r_2	r_1/r_2
2,6(m)-PyPBI–co–2,5(p)–PyPBI	1.084	0.626	1.73
3,5(m)-PyPBI–co–2,5(p)–PyPBI	0.779	0.593	1.31
2,4(m)-PyPBI–co–2,5(p)–PyPBI	2.02	1.13	1.79

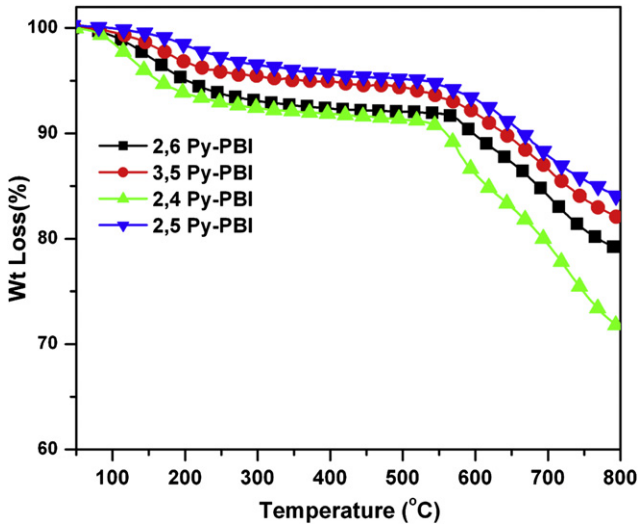

Fig. 6. TGA curves of the PyPBI homopolymers.

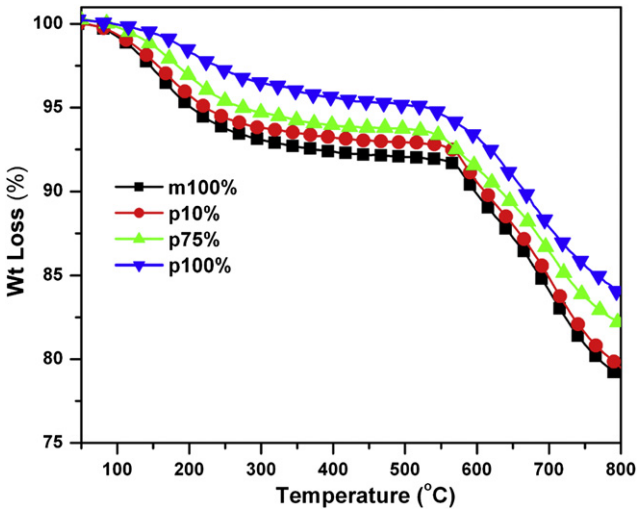

Fig. 7. TGA curves of the 2,6(m)-PyPBI-co-2,5(p)-PyPBI random copolymers. Para content (mol %) of the polymer indicated in the figure.

para content copolymer. In addition it is worth noting that the deviation in the para composition from the monomer feed (or anticipated composition) is not similar in all the three sets of copolymer despite the fact that in all the cases 2,5 PDA has been used as a para structure. These observations are quite unusual since in case of step polymerization, reactions are carried out close to 100% conversion for the synthesis of high molecular weight polymers. Also, step polymerizations are equilibrium reactions and in which reactivity of the functional groups are independent of chain length to which it is attached. Earlier few studies on copolycondensation showed the deviation in composition [17,46,47]. In our previous studies we have observed the similar behavior in case of meta-PBI-*co*-para-PBI. This deviation may be noticed due to the differences in monomer reactivates which in turn depend upon various structural factors like proximities of the functional groups and the solubility of the corresponding monomer. This suggests that probably the rates of the reactions of the monomers are not alike and hence the reactivity ratios of the monomers are different. Therefore, the deviation from the feed depends upon the structures of the monomers and this argument made it necessary for us to determine the reactivity ratios of the comonomers.

A simple kinetic scheme for copolymerization is used to discuss the rates of the reactions of the monomers. The M_1 and M_2 represent the para (2,5 PDA) and meta (2,6; 3,5; 2,4 PDAs) dibasic acid monomers, respectively. The asterisk in the prefix indicates the growing polymer chain. The four possible reaction sequences are following:

$$M_1^* + M_1 \overset{k_{11}}{\rightarrow} M_1M_1^*$$

$$M_1^* + M_2 \overset{k_{12}}{\rightarrow} M_1M_2^*$$

Table 4
Thermal stability data of all PyPBI homo polymers.

Homopolymer	W_{520} (%)[a]	T_{10} % (°C)[b]	W_{750} (%)[c]
2,5 PyPBI	95.25	668	85.62
3,5 PyPBI	94.16	641	83.75
2,6 PyPBI	92.16	596	80.96
2,4 PyPBI	91.25	560	75.06

[a] Residual weight percent at 520 °C.
[b] Temperature at which the 10% weight loss is observed.
[c] Residual weight percent at 750 °C.

$$M_2^* + M_1 \overset{k_{21}}{\rightarrow} M_2M_1^*$$

$$M_2^* + M_2 \overset{k_{22}}{\rightarrow} M_2M_2^*$$

The rate constants of the respective reactions are denoted by 'k' with appropriate sign in the suffix. We have calculated the reactivity ratio of three sets of PyPBI copolymers by applying Fineman–Ross [48] using the proton NMR data.

$$\frac{f_1(F_1 - F_2)}{f_2F_1} = \frac{F_2}{F_1}\left(\frac{f_1^2}{f_2^2}\right)r_1 - r_2 \qquad (4)$$

where f_1 and f_2 are the para and meta monomer mol fraction in the feed of the copolymerization, respectively. F_1 and F_2 are the instantaneous monomer mol fraction in the copolymer. A plot (Fig. 5) of equation (4) results in a straight line with slope equal to r_1 and intercept equal to $-r_2$, where r_1 (k_{11}/k_{12}) and r_2 (k_{22}/k_{21}) are the reactivity ratios of the monomer para (2,5 PDA) and, meta (2,4; 2,6 and 3,5 PDA), respectively. Table 3 lists reactivity ratios values

Table 5
Thermal stability data of 2,6(m)-co-2,5(p) PyPBI and 2,4(m)-co-2,5(p) PyPBI polymers.

Para content	W_{520} (%) [a]	T_{10} % (°C) [b]	W_{750} (%)[c]
2,6(m)-PyPBI-co-2,5(p)–PyPBI			
m 100%	92. 09	596	80.96
p 10%	92.87	609	81.59
p 25%	91.21	608	76.93
p 50%	95.02	650	83.14
p 75%	93.65	632	83.81
p 90%	92.98	632	84.03
p 100%	95.25	668	85.62
2,4(m)-PyPBI -co-2,5(p)–PyPBI			
m 100%	91.25	560	75.06
p 10%	92.73	581	77.63
p 25%	93.25	596	79.70
p 50%	93.25	595	80.48
p 75%	95.19	654	83.94
p 90%	94.15	645	83.07
p 100%	95.25	668	85.62

[a] Residual weight percent at 520 °C.
[b] Temperature at which the 10% weight loss is observed.
[c] Residual weight percent at 750 °C.

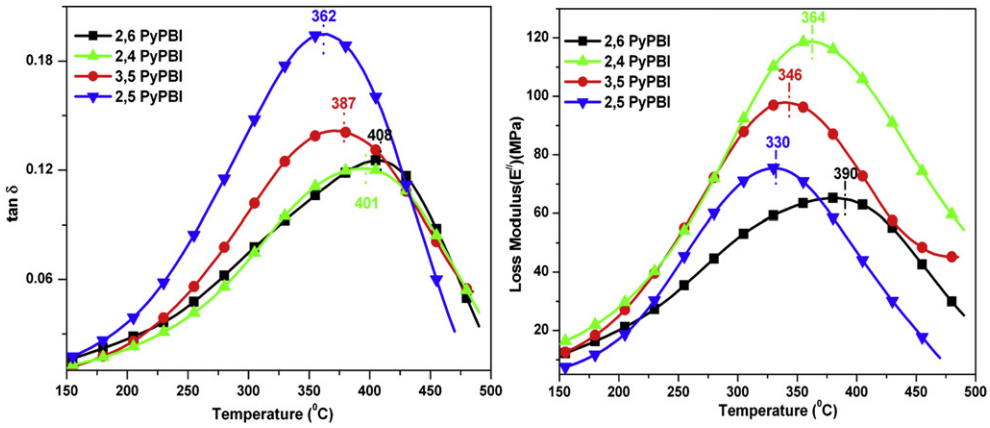

Fig. 8. DMA plots (tan δ and E″ against temperature) of PyPBI homopolymers. The vertical dotted lines shown in the plots represent the glass transition temperatures.

calculated by using equation (4) for all the three sets of PyPBI copolymer. Fig. 5 represents the Fineman–Ross for 2,4(m)-PyPBI-*co*-2,5(p)-PyPBI copolymer. The plots for the other two sets of PyPBI copolymer are presented in Supporting Information Figs. 9 and 10. Table 3 data clearly indicates that in all the three cases the reactivity ratio (r_1) of para monomer (2,5 PDA) is higher than the reactivity ratio (r_2) of its meta counter parts. This attributes that the reactivity of para monomer is higher than the meta monomers. The higher reactivity is due to lower solubility of para in the PPA medium and hence we obtained higher molecular weight polymers (Table 1) with increasing para content in the polymer backbone. The higher reactivity of para explains the positive deviation from the feed of the monomer (Table 2). It is also interesting to note that the values of the reactivity ratios (r_1/r_2) for three sets are not similar. In Table 2, also we have observed the similar behavior, where the deviations of the copolymer composition from the feed are not similar; instead it depends on the monomer pairs. Therefore, these results attributes to the fact that the reactivity of para monomer (2,5 PDA) depends upon not only by its low solubility in the polymerization medium (PPA medium) but it also can be tuned by choosing appropriate counter part.

3.4. Thermal stability study

The remarkably high thermal stability owing to the rigidity of PBI types polymers are well known and have been addressed by many authors in the literature [10,17,25,29]. In our previous publication we have shown that the thermal stability of m-PBI-*co*-p-PBI enhances significantly with increasing para content in the copolymer. The TGA studies of all the PyPBI copolymer samples are performed under nitrogen atmosphere at a heating rate of 10 °C/minute. TGA curves of all homo PyPBI copolymers are shown in the Fig. 6 and the thermal stability data obtained from the Fig. 6 for all the homopolymers are presented in the Table 4. Two distinct weight losses are observed: initial weight loss at around 100–120 °C and the second weight loss at around 520–540 °C. The initial weight loss is due to the loss of loosely bound absorbed water molecule. Despite of exhaustive drying in vacuum oven at 100 °C, PBI types of polymers can absorb ~5% (by weight) moisture very easily from the atmosphere during the sample handling time due to their hygroscopic nature. The presence of absorbed moisture also confirmed from O–H frequency seen in the IR spectra (Fig. 1) [43]. The degradation of the polymer backbone is seen at ~520–540 °C. Fig. 6 and Table 4 data suggest that < 10% weight loss is observed at 520 °C, indicating the very high thermal stability of these polymers. TGA curves and Table 4 data clearly suggest that the thermal stability of these homopolymers depends upon the isomeric structure of PDA. It must be noted that 2,5 PDA (the para structure) shows the highest thermal stability among the four. TGA curves of few representative samples of 2,6(m)-PyPBI-*co*-2,5(p)-PyPBI copolymer are shown in Fig. 7. The TGA curves for the other two sets of copolymers, 2,4(m)-PyPBI-*co*-2,5(p)-PyPBI and 3,5(m)-PyPBI-*co*-2,5(p)-PyPBI are presented in Supporting Information Figs. 11 and 12, respectively. Table 5 represents thermal stability data of PyPBI copolymers. From all these TGA curves and Table 5 data, it is very much clear that the thermal stability of the copolymer increases with increasing para content. Hence, we can

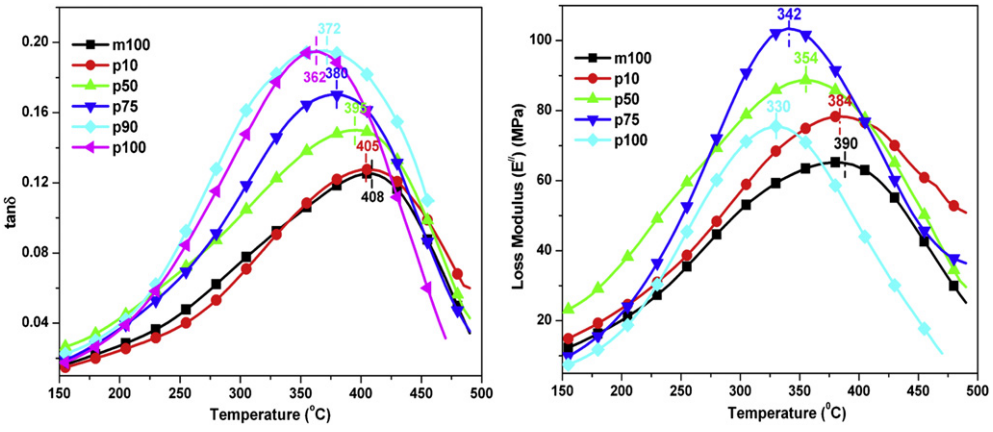

Fig. 9. DMA plots (tan δ and E″ against temperature) of 2,6(m)-PyPBI-*co*-2,5(p)-PyPBI copolymers. The T_g s are shown in the figure by vertical dotted lines.

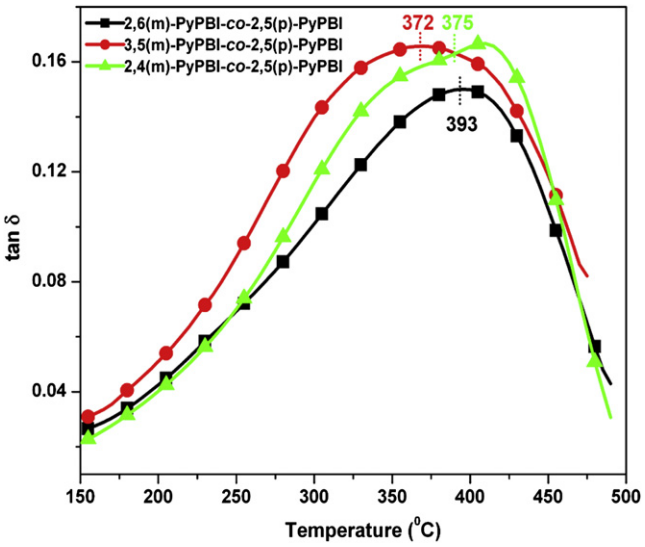

Fig. 10. Comparison of Tg s of 50% para content sample of three different copolymers obtained from the tan δ vs temperature plot.

conclude that the introduction of para pyridine linkage in the polymer backbone significantly influences and enhances the thermal stability of the PyPBI random copolymers. Another important observation must be noted that the thermal stability behavior of these copolymers depends on the monomer pairs, for example the temperature at which the 10% weight loss is observed for the 50% para content sample in case of 2,6(m)-PyPBI-*co*-2,5(p)-PyPBI copolymer is 650 °C where as the same is 595 °C in case of 2,4(m)-PyPBI-*co*-2,5(p)-PyPBI copolymer (Table 5). Hence the isomeric structure of PDA monomers influences the thermal stabilities of PyPBI copolymers.

3.5. Glass transition temperatures (T_g) of copolymers

The thermomechanical properties of all the pyridine homo and copolymers are studied by using a dynamical mechanical analyzer (DMA). The glass transition temperatures (T_g) of all the PyPBI homo and copolymers are obtained from the DMA study. The temperature at which the maximum in loss modulus and tan δ plot is observed that corresponds to the glass transition temperature (Tg). All the samples films are scanned in DMA from 150 °C to 500 °C at a heating rate of 5 °C/min. The storage modulus (E′), loss modulus (E″) and tan δ values are measured at a constant frequency of 5 Hz with a preload force of 0.01 N. We have carried out the DMA heating scan after the annealing the samples (films) at 150 °C for 30 min. Earlier studies on PBI blend system showed that the first DMA heating run results in a complicated structure because of the involvement of various processes such as removal of residual solvent, the glass transitions and the phase separation [49]. Also, it is proved from the I.R and TGA studies that the PBI is very hygroscopic in nature and can easily absorb ~5% (by weight) moisture from the atmosphere. The absorbed moisture may affect the mechanical properties and hence the glass transition temperature. Therefore, we have annealed the samples at 150 °C prior to the heating scan and we could obtain reproducible T_g from the DMA study for all the samples. The temperature dependent plot of tan δ and loss modulus (E″) for Py-PBI homopolymers, 2,6(m)-PyPBI-co-2,5(p)-PyPBI, 3,5(m)-PyPBI-co-2,5(p)-PyPBI and 2,4(m)-PyPBI-co-2,5(p)-PyPBI copolymers are presented in Figs 8 and 9, Supporting Information Figs. 13 and 14, respectively. In all the cases, the T_g obtained from the loss modulus plot is somewhat lower than that obtained from the tan δ plot. Earlier several author reported similar type difference in T_g from the two plots for various polymer system. In our discussion we will be dealing with the T_g s obtained from tan δ plots. However, it must be noted that the nature of variation of T_g from sample to sample in the copolymers are identical for both tan δ and E″ plots. The tan δ plots (Fig. 8) show that the glass transition temperature (Tg) of the 2,6(m)PyPBI, 2,4(m)PyPBI, 3,5(m) PyPBI, and 2,5(p)PyPBI homopolymers are 408, 401, 387 and 360 °C, respectively. Typically PBI polymer shows very high T_g (> 350 °C) [10,24,29]. So our values are in agreement with the reported values. To our knowledge until now no efforts have been made to measure the T_g of the PyPBI homopolymers. The above T_g values have two important implications: the T_g of the para structure PyPBI (2,5 PyPBI) is significantly lower (~40 °C) than all meta structure PyPBI (2,6; 3,5 and 2,4 PyPBI) and the T_g of PyPBI not only depends upon the meta–para structure but it also varies depending upon the position of carboxylic acid in the pyridine ring (isomeric effect). The lower T_g value attributes that the para structured PyPBI backbone is more flexible than the meta structured PyPBI. Our IR and Raman studies (described in the previous section) suggest the presence of better conjugation between the imidazole rings and para pyridine linkage in case of para PyPBI. Also, para structure PBI has a symmetrical backbone. The flexibility and symmetrical nature of the 2,5 PyPBI (para) homopolymer increases the segmental mobility of the chain and hence para structure shows a lower T_g compare to the meta structure [50]. Among the meta structure PyPBI homopolymer, the T_g of 3,5 PyPBI is lower (387 °C) compared to 2,6 and 2,4 PyPBI (408 and 401 °C). This is due to the position of carboxylic acid group in the pyridine moiety. The better symmetrical nature of 3,5 PyPBI than other two meta PyPBI is responsible for lower T_g of former compare to the other two meta PyPBIs.

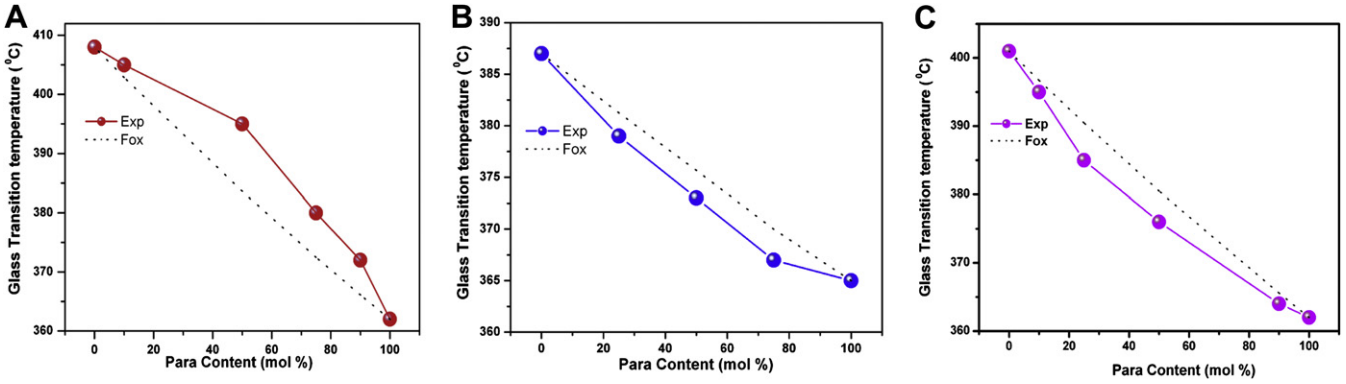

Fig. 11. Variation of glass transition temperature (T_g) with para content (mol %) of the PyPBI copolymers. Solid line is experimentally obtained from the tan δ vs temperature plots and dotted line is calculated from the Fox equation. (A) 2,6(m)-PyPBI-*co*-2,5(p)-PyPBI (B) 3,5(m)-PyPBI–*co*-2,5(p)- PyPBI (C) 2,4(m)-PyPBI-*co*-2,5(p)-PyPBI.

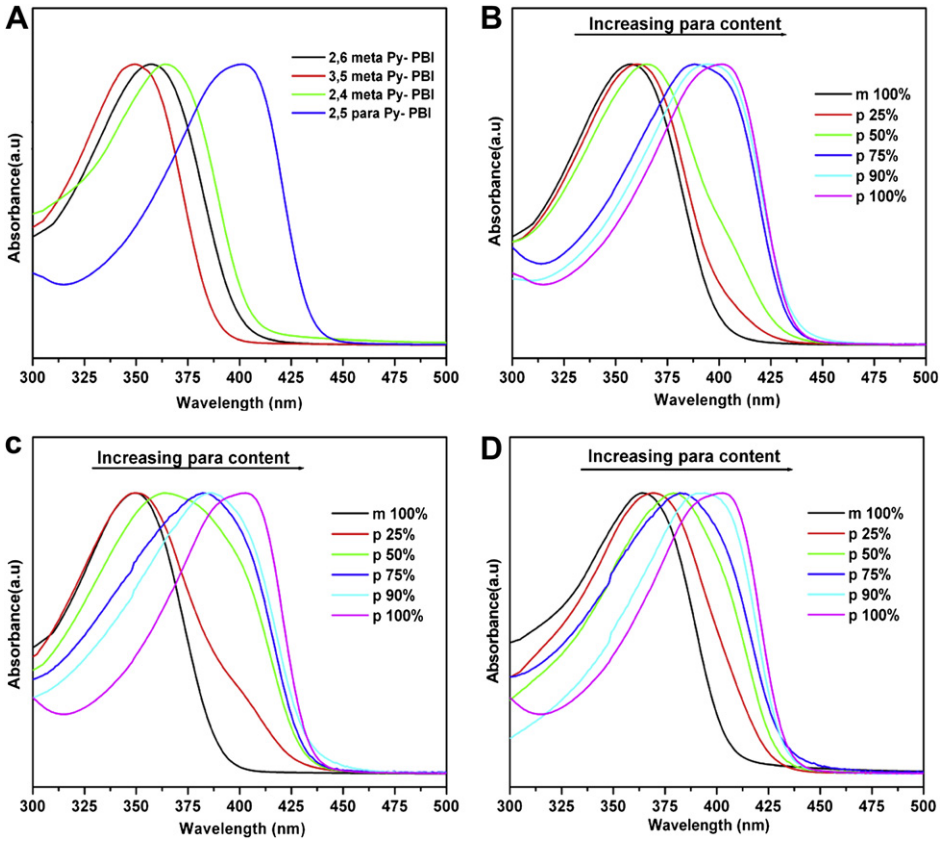

Fig. 12. Absorption spectra of the Py-PBI homo and copolymers polymers in DMAc solution as recorded with a cuvette of 1 cm path length. Concentrations are 2×10^{-5} M. (A) Py-PBI homo polymers (B) 2,6(m)-PyPBI-*co*-2,5(p)-PyPBI (C) 3,5(m)-PyPBI-*co*-2,5(p)-PyPBI (D) 2,4(m)-PyPBI-*co*-2,5(p)- PyPBI.

All the DMA plots of PyPBI copolymers (Fig. 9, Supporting Information Fig. 13 and Fig. 14) exhibit a single T_g. In all the three sets of copolymers, the T_g decreases with increasing para content as expected from their representative values for homopolymers. It is interesting to note that the T_g values of copolymers are highly dependent on the structure of the monomer pairs. Fig. 10 shows a comparison of T_g value for 50% para content copolymer of three different sets. Hence the T_g is controlled not only by the meta–para combination structure but also tuned by the different isomeric structure of meta PDAs. The variations of copolymer Tg s with para content (mol %) for three sets of copolymers are presented in Fig. 11. The expected T_g of the random copolymers are estimated by the Fox equation (Equation (5)) as follows:

$$\frac{1}{T_g} = \frac{w_1}{T_{g_1}} + \frac{w_2}{T_{g_2}} \tag{5}$$

where w_1 and w_2 are the weight fractions and T_{g1} and $T_{g2}$are the glass transition temperatures of the two homopolymers. Fig. 11 shows that the experimental T_g values obtained from the DMA measurements (solid line) are deviated from the calculated values obtained from the Fox equation (dotted line).Positive deviation obtained from the linear additive rule in case of 2,6(m)-PyPBI-*co*-2,5(p)-PyPBI where as other two sets copolymers exhibit the negative deviation from the Fox equation (Fig. 11). Among the three meta PDAs, the 2,6 PDA is the less symmetrical in nature which pushes two polymer chains away from each other owing to the interchain steric hindrance in case of 2,6(m)-PyPBI-*co*-2,5(p) PyPBI resulting a positive deviation from the expected T_g values. In other two sets of copolymers the negative deviation are observed due to the fact that in these two cases, the meta component PDAs (2,4 and 3,5) are more symmetrical and has some similarities with 2,5 PDA. The most important observation from the above study is that the dependence of T_g with para content depends upon with whom 2,5 PDA is being partnered. Hence the effect of isomeric structure of PDA on the flexibility of the PyPBI random copolymer is demonstrated.

Table 6
Electronic spectroscopy data of all the Py-PBI copolymers.

Copolymer	Para Content (mol %)	Absorption (λ_{max}) peak (nm)	Emission peak (nm)
2,6(m)-PyPBI-co–2,5(p)–PyPBI	0	355	411,430
	10	360	460
	25	362	460
	50	365	465
	75	390	448,466
	90	395	448,468
	100	400	448,468
3,5(m)-PyPBI-co–2,5(p)–PyPBI	0	350	424
	10	348	437
	25	352	464
	50	365	468
	75	382	468
	90	385	469
	100	400	448,468
2,4(m)-PyPBI-co–2,5(p)–PyPBI	0	365	450
	10	365	460
	25	370	463
	50	380	465
	75	383	467
	90	395	468
	100	400	448,468

3.6. Spectroscopy

The absorption and the fluorescence emission spectra of all the PyPBI homo and copolymers are studied from their dilute solution (2×10^{-5} M) in dimethyl acetamide (DMAc). The concentration is expressed by considering one repeat unit as one mol PyPBI. The absorption spectra of PyPBI homo and three sets of PyPBI copolymers in DMAc are shown in the Fig. 12. All the polymers exhibit very distinct $\pi \rightarrow \pi^*$ transition peak above 350 nm. The absorbance maximum (λ_{max}) peak positions are presented in the Table 6. Fig. 12 and Table 6 exhibit that the λ_{max} for $\pi \rightarrow \pi^*$ transition varies depending on the positions of carboxylic acids in the pyridine ring. Hence the isomeric effect of PDA on the conjugation of the PBI backbone is demonstrated. Table 6 data suggests the increasing conjugation order as follows: 2,5 > 2,4 > 2,6 > 3,5 and the λ_{max} of para structure (2,5) is ~50 nm higher than the others. This indicates that para is much more conjugated and all others have similar type conjugation. The observation is in good agreement with our other studies. A gradual bathochromic shift of the $\pi \rightarrow \pi^*$ absorbance maximum was observed in all the copolymers (Fig. 12) with increasing para content. We have noticed a similar observation to our previous work on m-PBI-*co*-p-PBI where the 100% para homopolymer absorbs at ~50 nm higher wavelengths than the 100% meta homopolymer. The introduction of the para linkage into the polymer backbone enhances the conjugation between the imidazole and the pyridine ring which results in the above mentioned bathochromic shift of the $\pi \rightarrow \pi^*$ absorption maxima. So our argument about the increased conjugation in the backbone due to the para substitution using IR spectra and Raman studies discussed in the previous sections are in good agreement with the absorption studies.

Earlier, it has been shown that all PBI types of heterocyclic polymers exhibit fluorescence emission and various phenomenon of PBI such as aggregation, gelation, conformational transition and sensing of halide ions have been explained by the help of fluorescence spectroscopy [19,21,26]. Therefore, it is very important to understand the photophysical behavior of the PyPBI polymer as we introduced the pyridine moiety in the polymer backbone which has potential to act as cationic sensor material. To our knowledge until now no such efforts have been made to study the photophysical behavior of the PyPBI type polymers. The emission spectra of the PyPBI homo and copolymers recorded in DMAc and are presented in the Fig. 13. The excitation wavelengths (λ_{exc}) are chosen based on the $\pi \rightarrow \pi^*$ absorption maxima shown in the Table 6. The concentrations of the solutions are 2×10^{-5} M and kept constant for all the cases. 2,6 PyPBI and 2,5 PyPBI exhibit two fluorescence bands, however the other two homopolymers (3,5 and 2,4 PyPBI) show only one fluorescence band with a very broad shoulder at the lower wavelength side which is almost undetectable (Fig. 13). Earlier, it was shown that PBI has two emission bands in which the lower and longer wavelength bands from the excited ^1L_b state in the benzimidazole ring of PBI are assigned as 0–0 and 0–1 transition respectively. Table 6 and Fig. 13 indicate that the para structure PyPBI emits at higher wavelength than the meta structure PyPBI. Among the meta structure PyPBI, the 2,4 PyPBI emits towards higher wavelength, indicating that the position of carboxylic acid in the pyridine ring (isomeric effect) control the conjugation in the

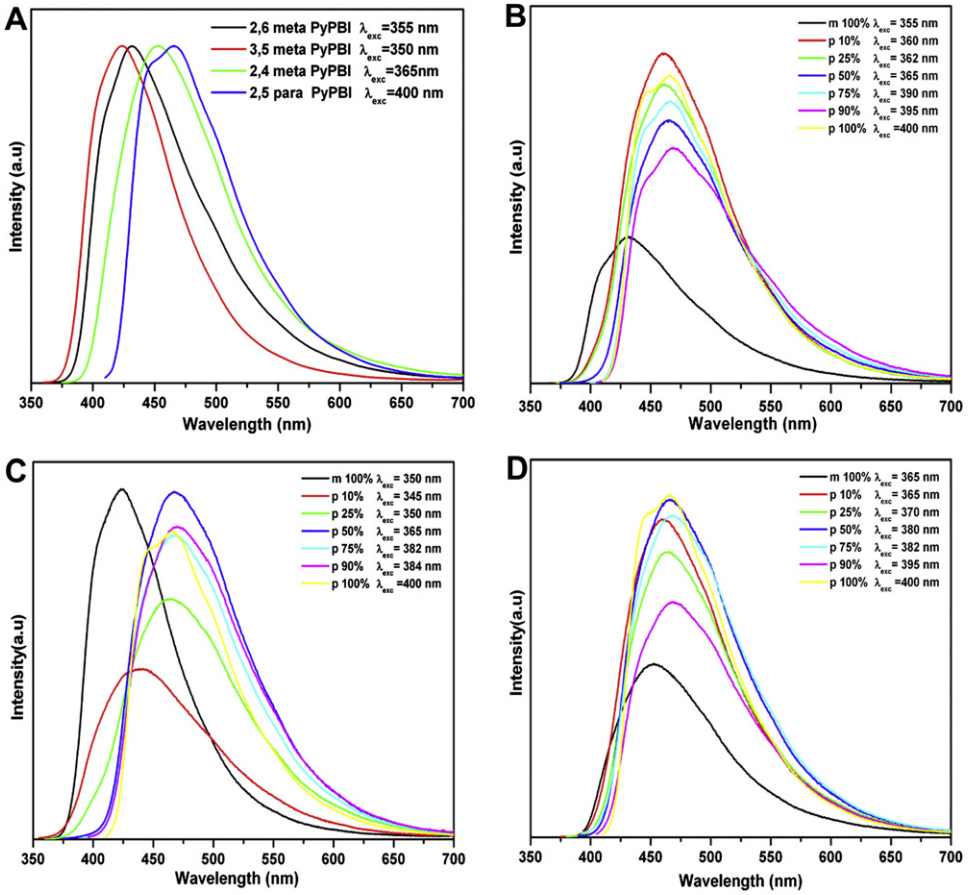

Fig. 13. Fluorescence emission spectra of the Py-PBI homo and copolymers in DMAc solution. Concentrations are identical to Fig. 13. Excitation wavelengths (λ_{exc}) are indicated in the figure. (A) Py-PBI homo polymers (B) 2,6(m)-PyPBI-*co*-2,5(p)-PyPBI (C) 3,5(m)-PyPBI-*co*-2,5(p)-PyPBI (D) 2,4(m)-PyPBI-*co*-2,5 (p) PyPBI.

polymer backbone. All the three types of copolymer pairs the emission bands are shifted gradually to the higher wavelength with increasing para content (Fig. 13 and Table 6). The shifting of the emission bands towards the longer wavelength also supports the conjugation along the polymer backbone due to the introduction of the para pyridine linkages. This observation once again strengthens our previous argument about the better conjugation of higher para content copolymers.

4. Conclusions

We have synthesized and studied various molecular properties of three different sets of polybenzimidazole random copolymers consisting of meta and para pyridine linkages in the backbone. In all the cases the higher para content copolymer yielded higher molecular weight polymers owing to low solubility of para structure 2,5 pyridine dicarboxylic acid (2,5 PDA) in the polymerization medium. FT-IR and Raman spectroscopy studies demonstrate the increase of conjugation along the polymer chain for higher para content polymers. The para structure 2,5 PDA has the higher reactivity than all other meta structure PDAs and most importantly the reactivity of 2,5 PDA varies depending upon with which meta PDA it forms the copolymer pair. In all the three sets of copolymers the thermal stabilities are increased with increasing para content in the copolymers. The position of the carboxylic acid groups in the pyridine ring of PDA monomers influences the T_g of the PyPBI homo and copolymers. The nature of deviations of T_g of copolymers from the expected T_g (as per the Fox equation) are not similar in three cases, attributing the influence of isotopic structures of monomers. The absorption maxima and the emission wavelength are shifted towards the higher wavelength with increasing para content in the polymer provide the proof for increased conjugation. In summary, we have demonstrated the effect of structural isomers of PDA monomers on the copolymerization and the various molecular properties of PyPBI random copolymers.

Acknowledgements

We gratefully acknowledge financial support by DST (Grant number SR/S1/PC-58/2008). We thank Mr. Arun Kr. Bar and Ritwik Samanta for helping us with the FT-Raman and NMR experiments, respectively. A.S. thanks CSIR for the senior research fellowship.

Appendix. Supplementary material

Supplementary data related to this article can be found online at doi:10.1016/j.polymer.2010.10.013.

References

[1] Fuel cell handbook. 6th ed. EG & G Technical Services, Inc. U.S. Department of Energy; November 2002.
[2] Rikukawa M, Sanui K. Prog Polym Sci 2000;25(10):1463–502.
[3] Hickner MA, Ghassemi H, Kim SY, Einsla BR, McGrath JE. Chem Rev 2004;104 (10):4587–612.
[4] Higashihara T, Matsumoto K, Ueda M. Polymer 2009;50(23):5341–57.
[5] Bouchet R, Siebert E. Solid State Ionics 1999;118(3–4):287–99.
[6] Ma YL, Wainright JS, Litt MH, Savinell RF. J Electrochem Soc 2004;151(1):A8–16.
[7] Li Q, Jensena JO, Savinell RF, Bjerrum NJ. Prog Polym Sci 2009;34(5):449–77.
[8] Mader J, Xiao L, Schmidt TJ, Benicewicz BC. Adv Polym Sci 2008;216:63–124.
[9] Lobato J, Cañizares P, Rodrigo MA, Linares JJ, Manjavacas GJ. Membr Sci 2006;280(1–2):351–62.
[10] Neuse EW. Adv.Polym Sci 1982;47:1–42.
[11] Asensio JN, Borrós S, Gómez- Romero P. J Electrochem Soc 2004;151(2): A304–10.
[12] Xiao L, Zhang H, Jana T, Scanlon E, Chen R, Choe EW, et al. Fuel Cells 2005;5 (2):287–95.
[13] Jouanneau J, Mercier R, Gonon L, Gebel G. Macromolecules 2007;40(4):983–90.
[14] Li XZ, Liu JH, Yang SY, Huang SH, Lu JD, Pu JL. J Polym Sci. Part A Polym Chem 2006;44(19):5729–39.
[15] Chen CC, Wang LF, Wang JJ, Hsu TC, Chen CF. J Mater Sci 2002;37(19): 4109–15.
[16] Pu H, Wang L, Pan H, Wan D. J Polym Sci. Part A Polym Chem 2010;48(10): 2115–22.
[17] Sannigrahi A, Arunbabu D, Sankar RM, Jana T. J Phys Chem B 2007;111(42): 12124–32.
[18] Qing S, Huang W, Yan D. Euro Poly J 2005;41(7):1589–95.
[19] Kojima T. J Polym Sci. Polym Phys Ed 1980;18(8):1685–95.
[20] Shogbon CB, Brousseau JL, Zhang H, Benicewicz BC, Akpalu Y. Macromolecules 2006;36(26):9409–18.
[21] Sannigrahi A, Arunbabu D, Sankar RM, Jana T. Macromolecules 2007;40(8): 2844–51.
[22] Musto P, Karasz FE, MacKnight WJ. Macromolecules 1991;24(17):4762–9.
[23] Deimede V, Voyiatzis GA, Kallitsis JK, Qingfeng L, Bjerrum NJ. Macromolecules 2000;33(20):7609–17.
[24] Arunbabu D, Sannigrahi A, Jana T. J Phys Chem B 2008;112(17):5305–10.
[25] Choe EW, Choe DD. In: Salamone JC, editor. Polymeric materials encyclopedia. New York: CRC Press; 1996.
[26] Ghosh S, Sannigrahi A, Maity S. J Phys Chem B 2010;114(9):3122–32.
[27] Pu HT, Liu QZ, Liu GH. J Membr Sci 2004;241(2):169–75.
[28] Klaehn JR, Luther TA, Orme CJ, Jones MG, Wertsching AK, Peterson ES. Macromolecules 2007;40(21):7487–92.
[29] Sannigrahi A, Ghosh S, Lalnuntluanga J, Jana T. J Appl Polym Sci 2009;111 (5):2194–203.
[30] Li Q, He R, Jensen JQ, Bjerrum NJ. Chem Mater 2003;15(26):4896–915.
[31] Savinell R, Yeager E, Tryk D, Landau U, Wainright J, Weng D, et al. J Electrochem Soc 1994;141(4):L46–8.
[32] Weng D, Wainright JS, Landau U, Savinell RF. J Electrochem Soc 1996;143 (4):1260–3.
[33] Xiao L, Zhang H, Scanlon E, Ramanathan LS, Choe EW, Rogers D, et al. Chem Mater 2005;17(21):5328–33.
[34] Sannigrahi A, Arunbabu D, Jana T. Macromol Rapid Commun 2006;27(22): 1962–7.
[35] Li Q, Pan C, Jensen JO, Noye' P, Bjerrum NJ. Chem Mater 2007;19(3):350–2.
[36] Yu S, Benicewicz BC. Macromolecules 2009;42(22):8640–8.
[37] Quartarone E, Magistris A, Mustarelli P, Grandi S, Carollo A, Zukowska GZ, et al. Fuel Cells 2009;9(4):349–55.
[38] Shao H, Shi Z, Fang J, Yin J. Polymer 2009;50(25):5987–95.
[39] Wang K-L, Liou W-T, Liaw D-J, Huang S-T. Polymer 2008;49(6):1538–46.
[40] Yu S, Zhang H, Xiao L, Choe EW, Benicewicz BC. Fuel Cells 2009;9(4):318–24.
[41] Apelblat A, Manzurola E, Balal NA. J Chem Thermodyn 2006;38(5):565–71.
[42] Long BW, Wang LS, Wu JS. J Chem Eng Data 2005;50(1):136–7.
[43] Brooks NW, Duckett RA, Rose J, Ward IM, Clements J. Polymer 1993;34(19): 4038–42.
[44] Silverstein RM, Webster FX. Spectroscopic identification of organic compounds. NY: John Wiley & Sons Inc.; 2002.
[45] Li Q, He R, Berg RW, Hjuler HA, Bjerrum NJ. SolidState Ionics 2004;168(1–2): 177–85.
[46] Lyoo WS, Kim JH, Ha WS. J Appl Poly Sci 1996;62(3):473–80.
[47] Sundarrajan S, Ganesh K, Srinivasan KSV. Polymer 2003;44(1):61–71.
[48] Fineman M, Ross SD. J Polym Sci 1950;5(2):259–62.
[49] Liang K, Bánhegyi G, Karasz FE, MacKnight WJ. J Polym Sci. Part B Polym Phys 1991;29(6):649–57.
[50] Sperling LH. Introduction to physical polymer science. NY: John Wiley & Sons Inc.; 1992.